Electronic Supplementary Material (ESI) for Journal of Materials Chemistry A.

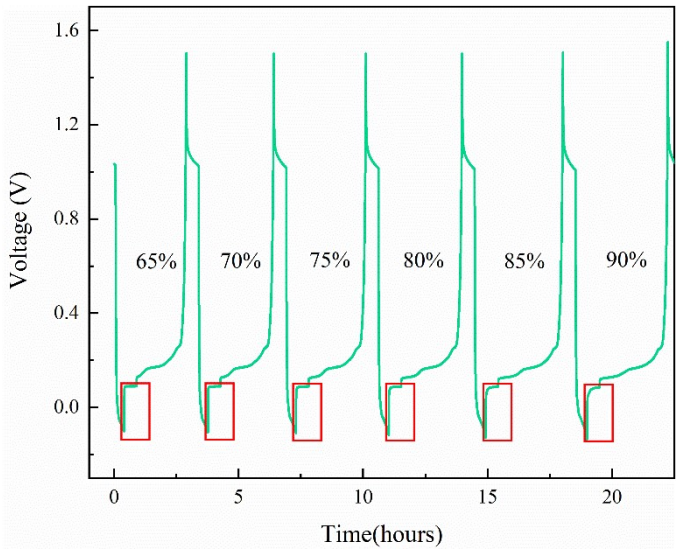

Figure S1. The representative cycling procedure to generate OCV data at various SOCs at 2C. At every SOC, the cell was lithiated to targeted SOC at 2C, rested for 30 minutes, delithiated to 1.5V at C/10, and rested for 30 minutes before next lithiation cycle. The evolution of relaxation voltages in red square is recorded and used for OCV analysis.

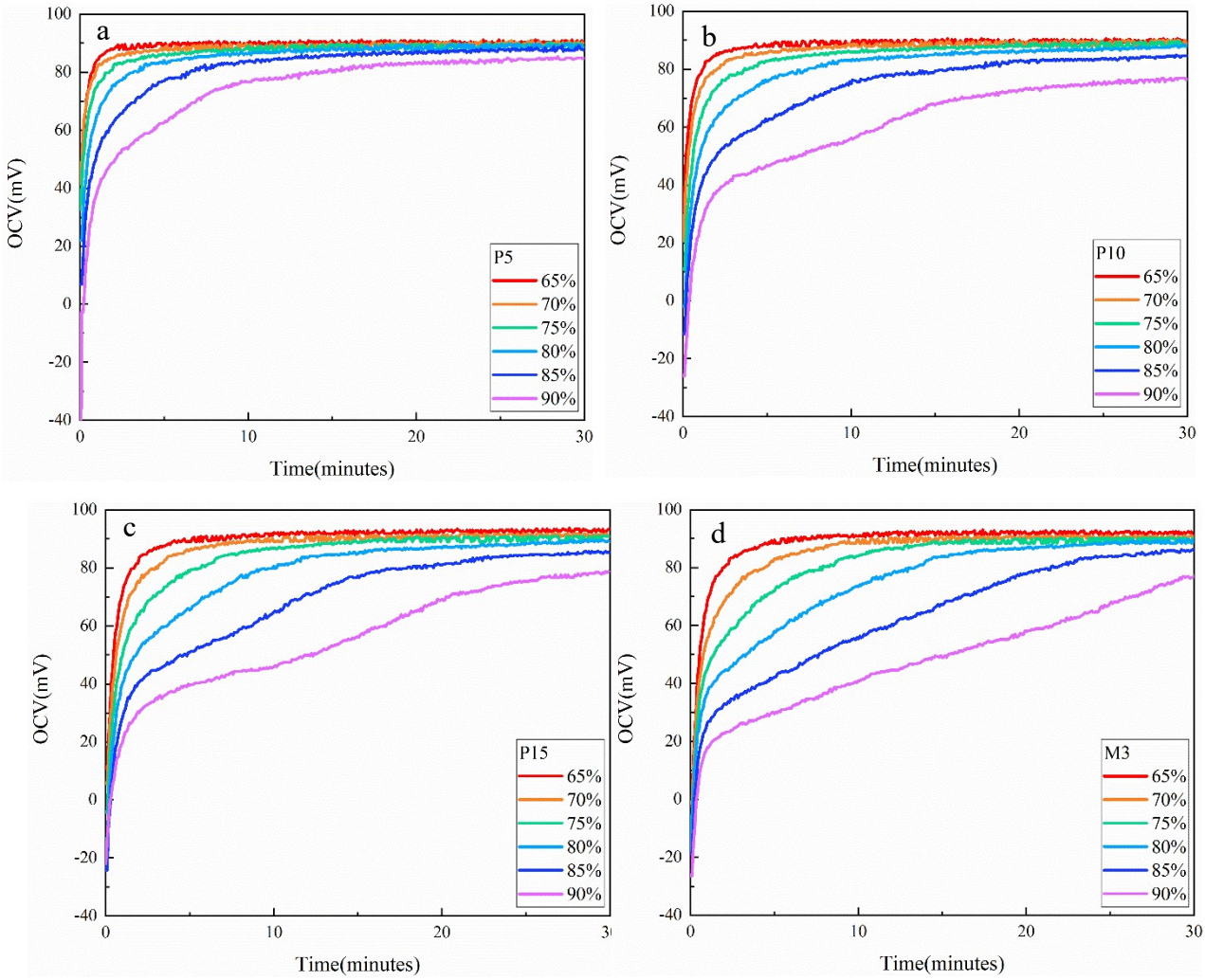

Figure S2. The OCV profiles of cells with P5 (a), P10 (b), P15 (c) and M3 (d) graphite anodes discharged to various SOCs at 2C. The OCV data were extracted from cycling data in **Figure S1**.

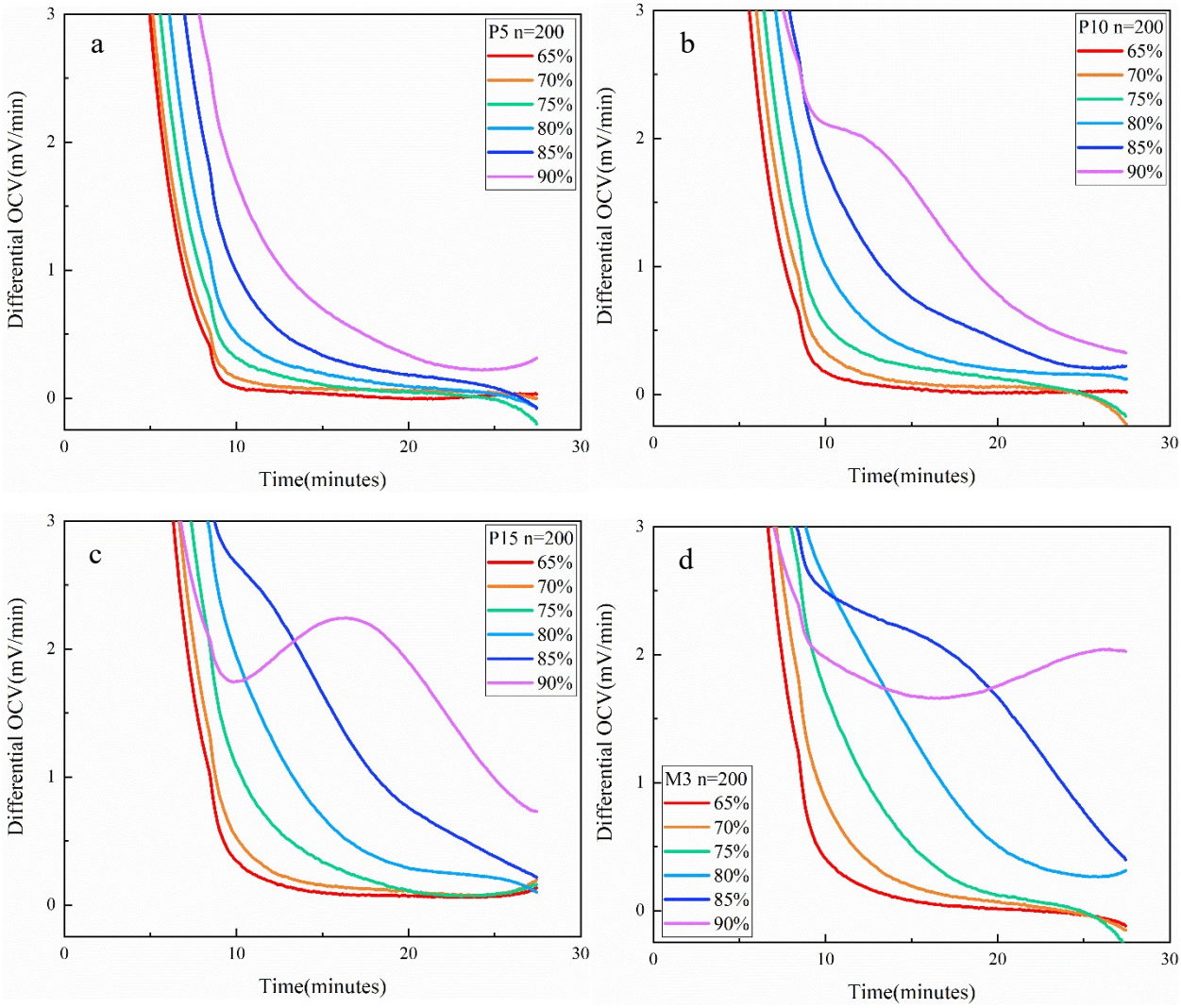

Figure S3. The differential OCV profiles in **Figure S2** of cells with P5 (a), P10 (b), P15 (c) and M3 (d) graphite anodes.

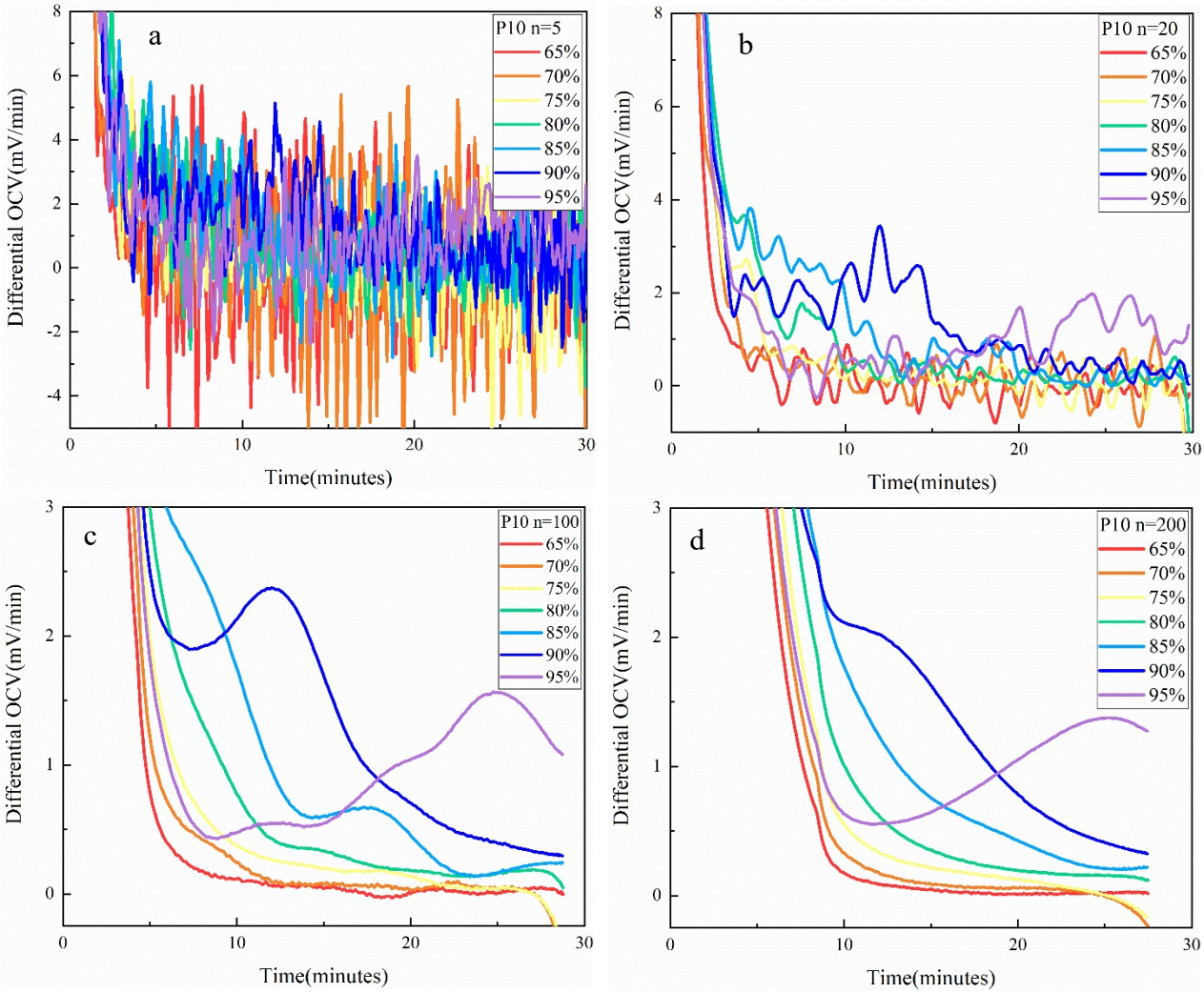

Figure S4. The dependence of dOCV peak clarity on the length of window (**n)** in MATLAB's smoothdata(). The dOCV profiles from **Figure S2b** are used as a representative to show the effect of **n**. When **n** = 200, the smoothed profile has the peak shape similar to that obtained at **n** = 20.

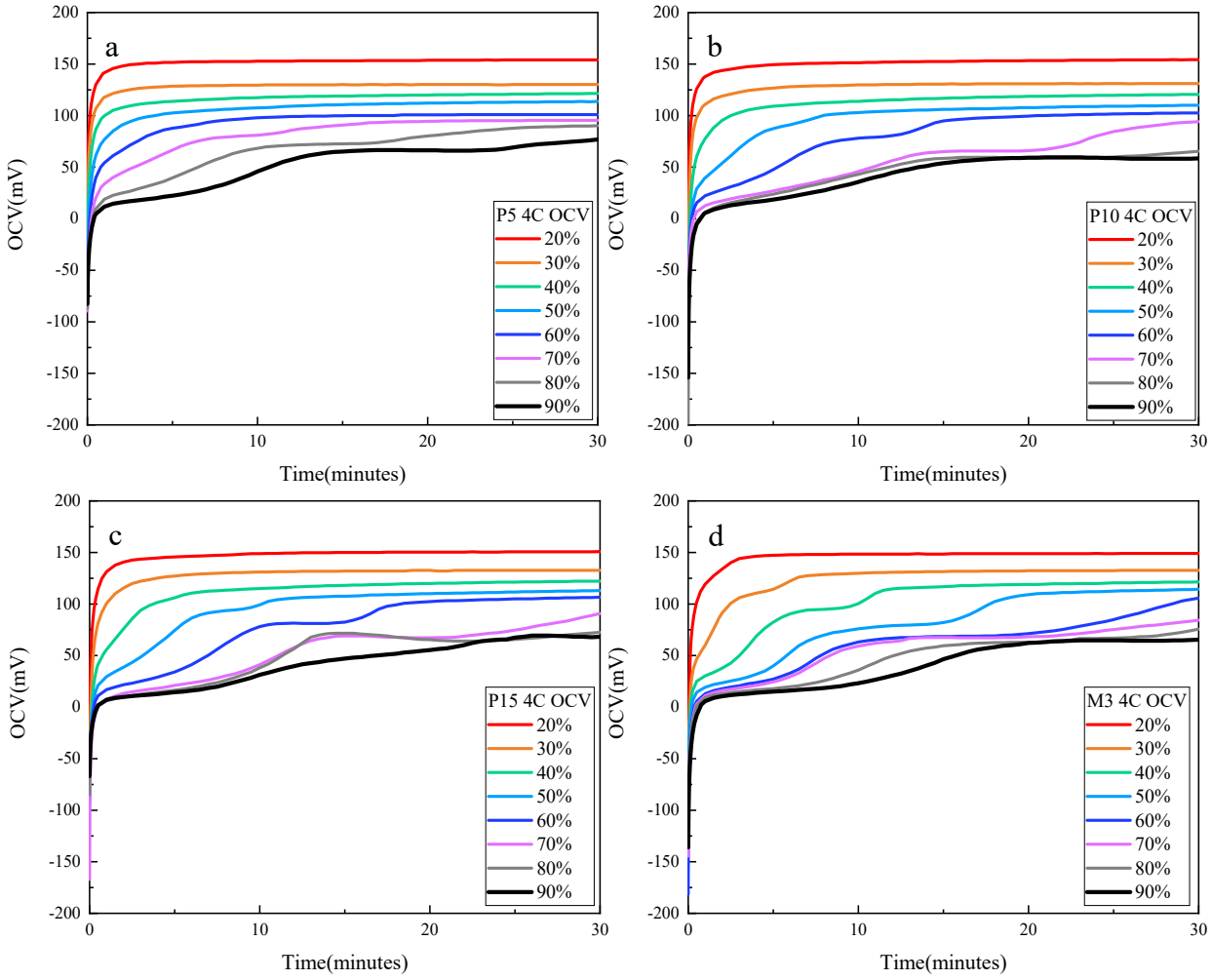

Figure S5. The OCV profiles of cells with P5 (a), P10 (b), P15 (c) and M3 (d) graphite anodes discharged to various SOCs at 4C.

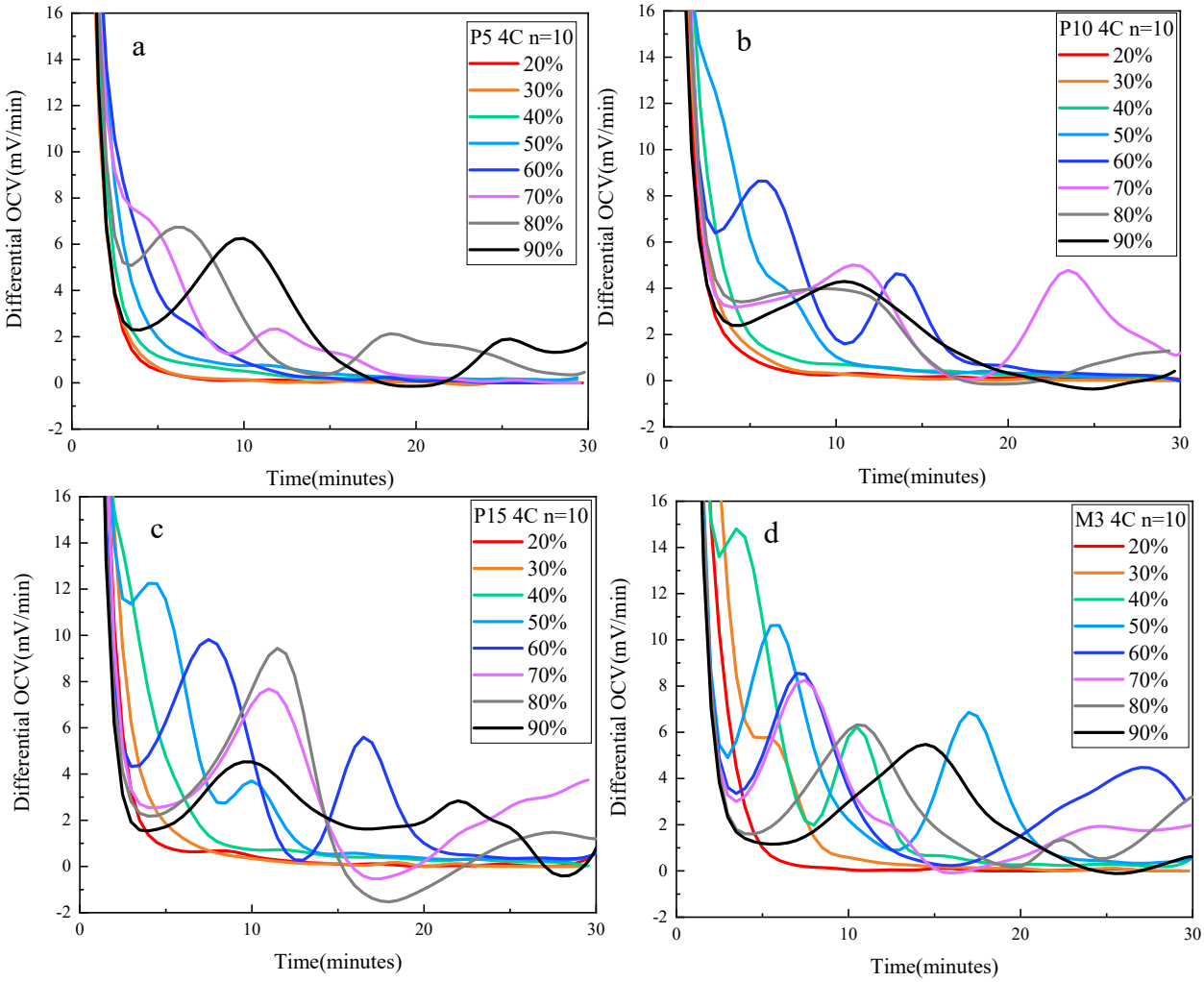

Figure S6. The differential OCV profiles in **Figure S5** of cells with P5 (a), P10 (b), P15 (c) and M3 (d) graphite anodes.

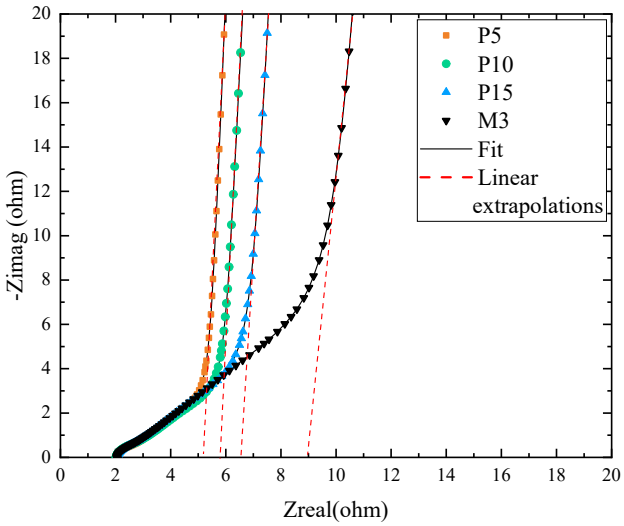

Figure S7. The Nyquist plots of symmetric cells with graphite electrodes. The intercept of extrapolation of low-frequency tail (red dashed lines) with real axis denotes the total resistance (R_{total}). The intercept of curves with the real axis represents the contact resistance ($R_{contact}$).

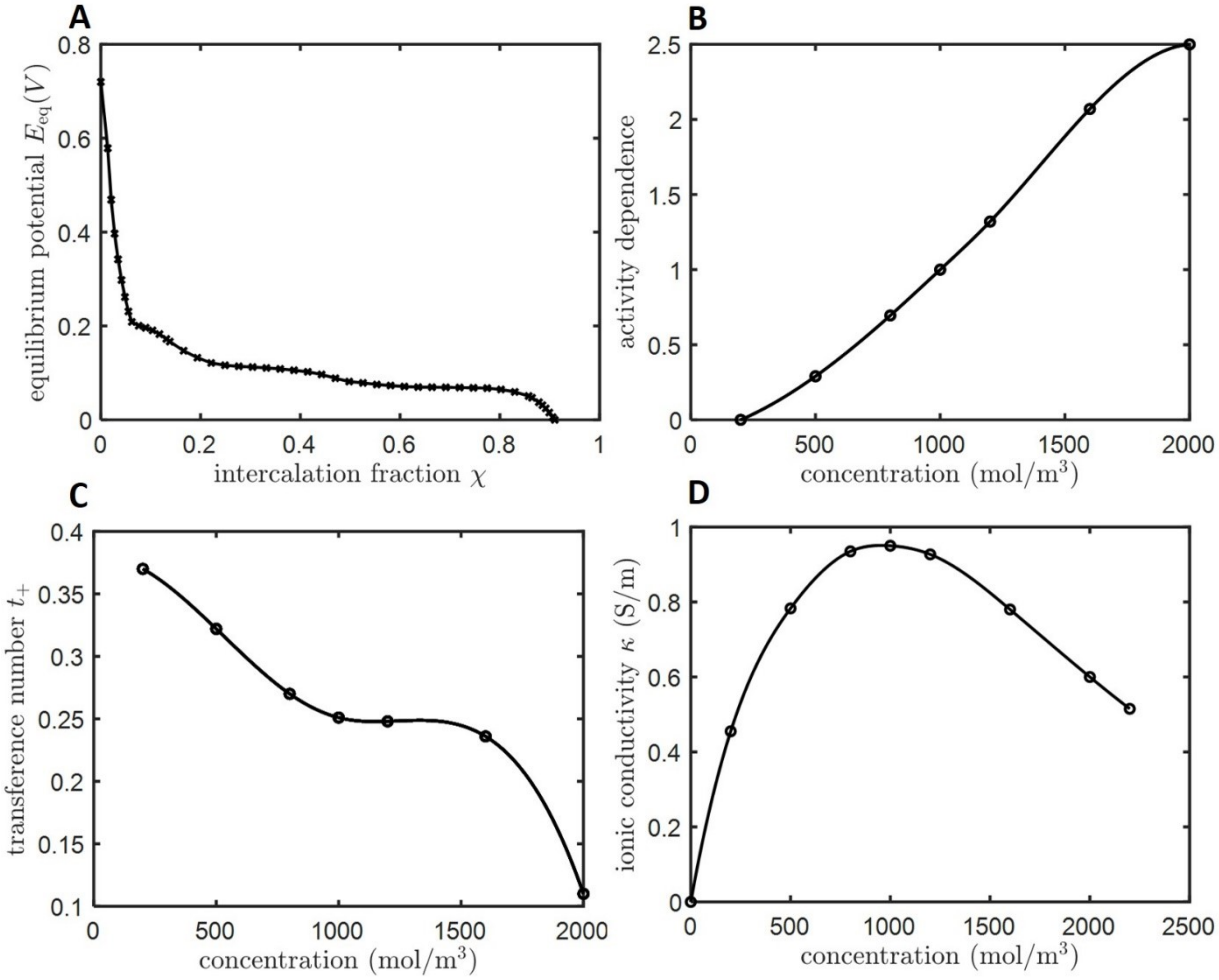

Figure S8: Material properties used in simulations of mono- and tri-layered graphite anode half-cells. A. Graphite equilibrium potential function. B. Ionic conductivity κ C. transference number $t+$ and D. activity coefficient as a function of Li^+ concentration c.

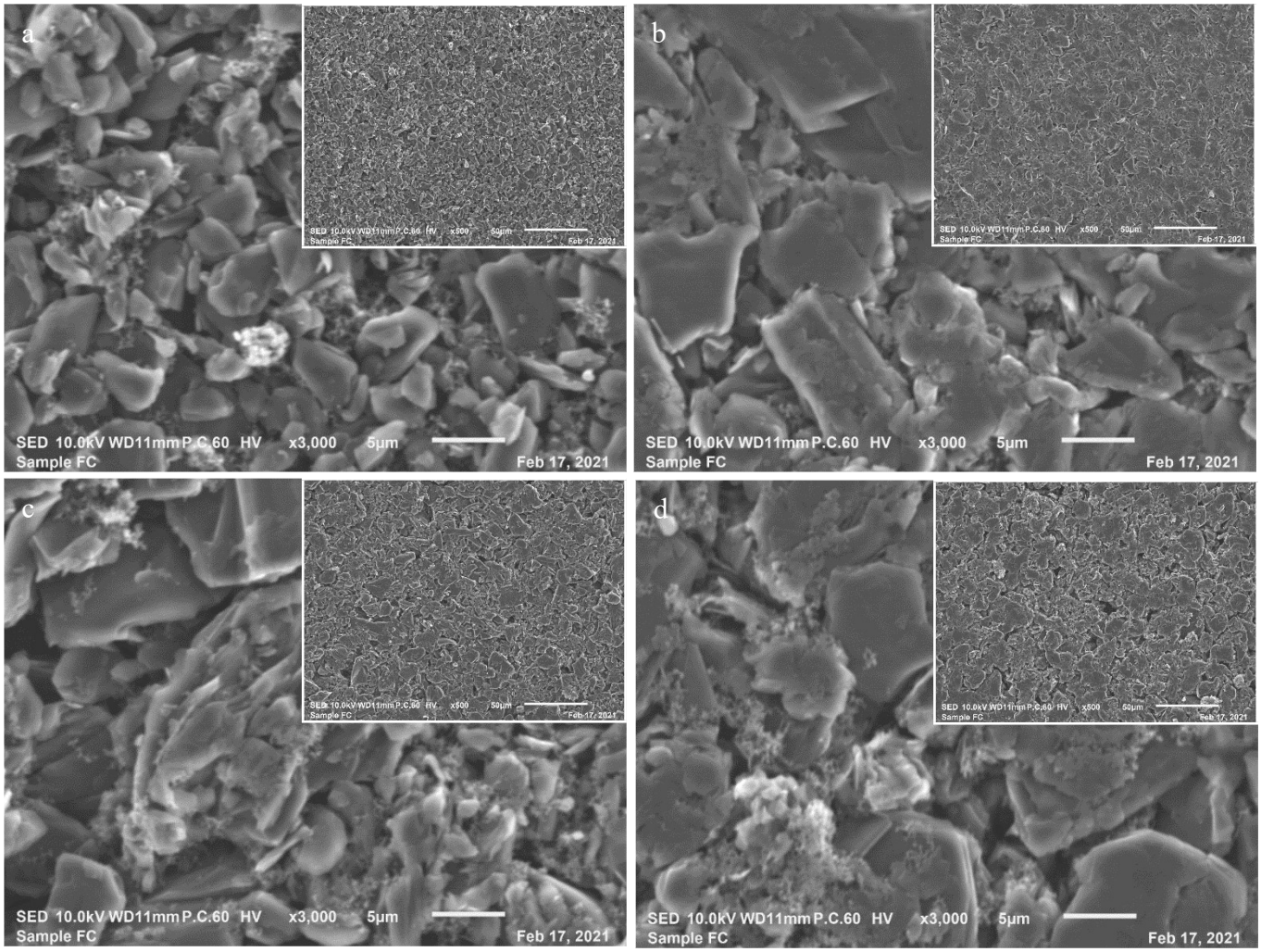

Figure S9. SEM images of pristine electrodes with P5 (a), P10 (b), P15 (c) and M3 (d) graphite.

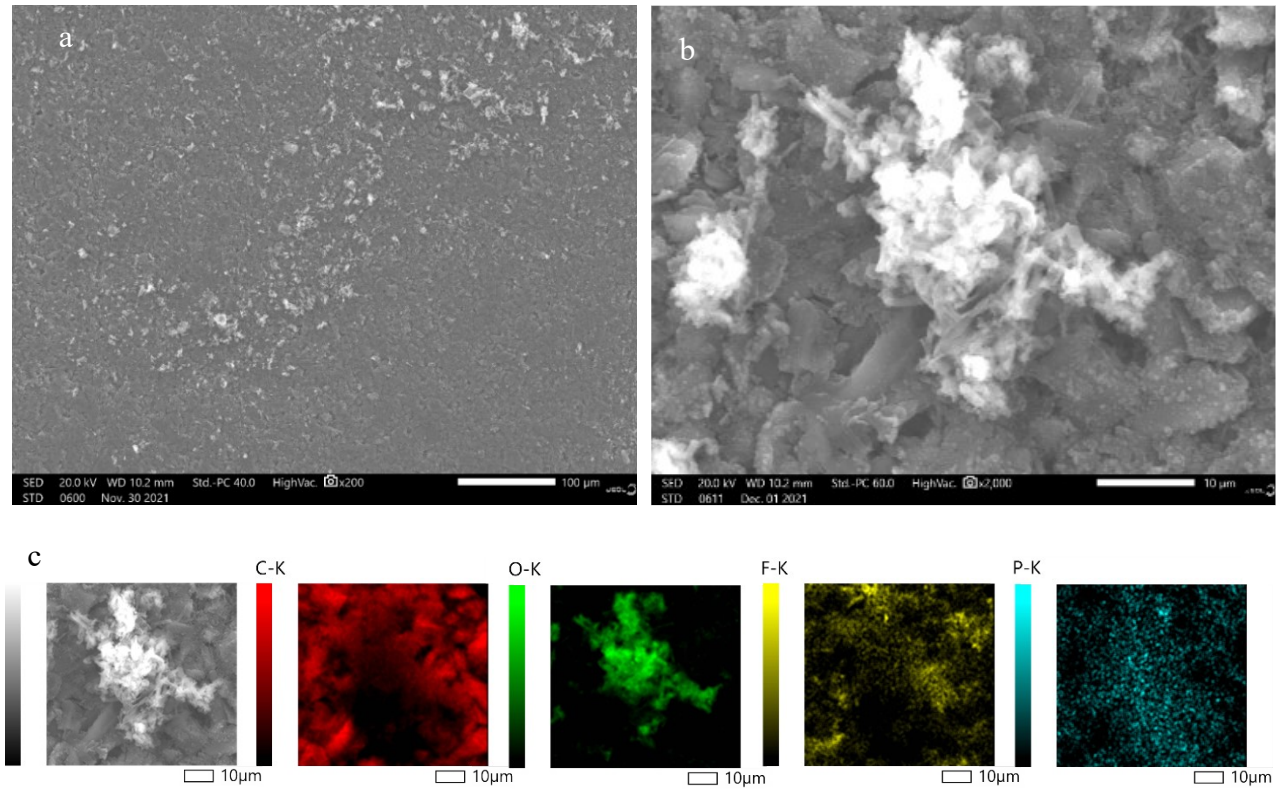

Figure S10. SEM images (a, b) and EDS mapping (c) of the cycled electrode with P10 graphite. Before disassembly, all cells underwent rate tests lithiated to 90% SOC at 2C and were charged to 1.5 V.

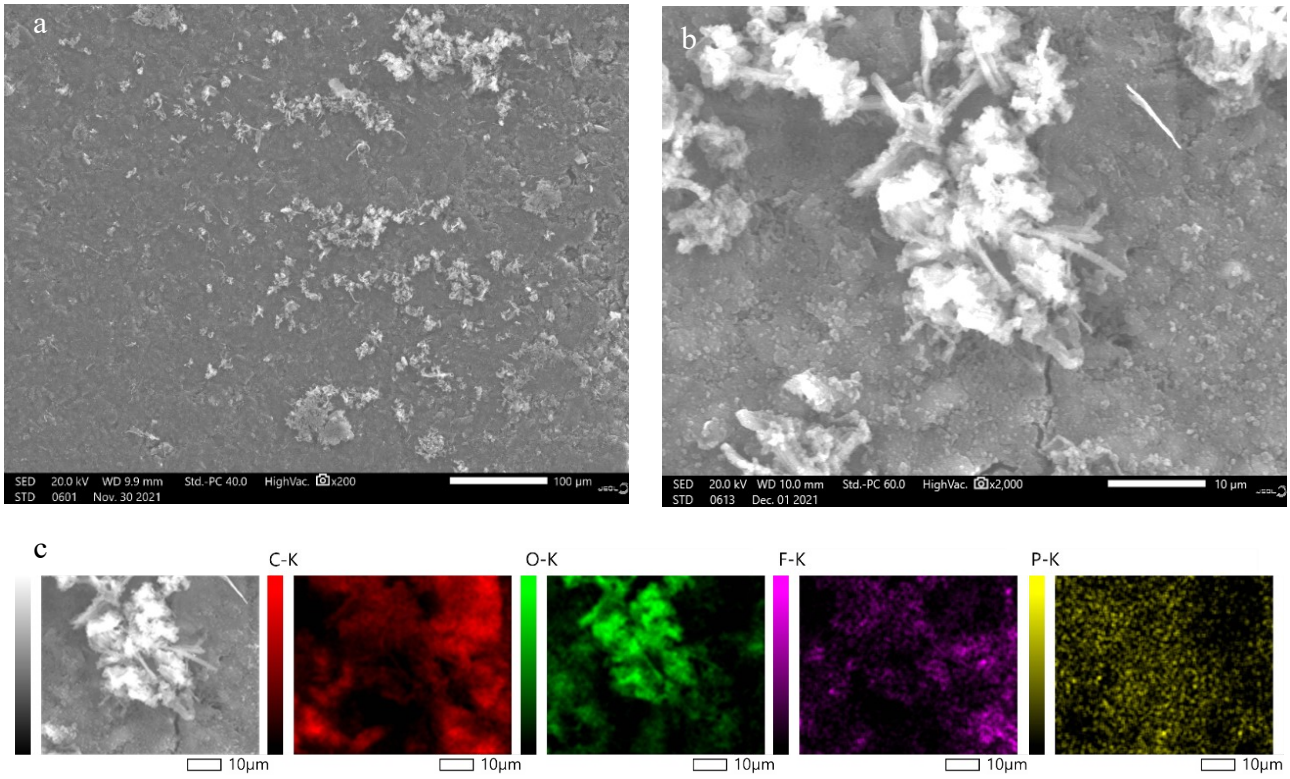

Figure S11. SEM image (a, b) and EDS mapping (c) of the cycled electrode with P15 graphite. Before disassembly, all cells underwent rate tests lithiatied to 90% SOC at 2C and were charged to 1.5 V

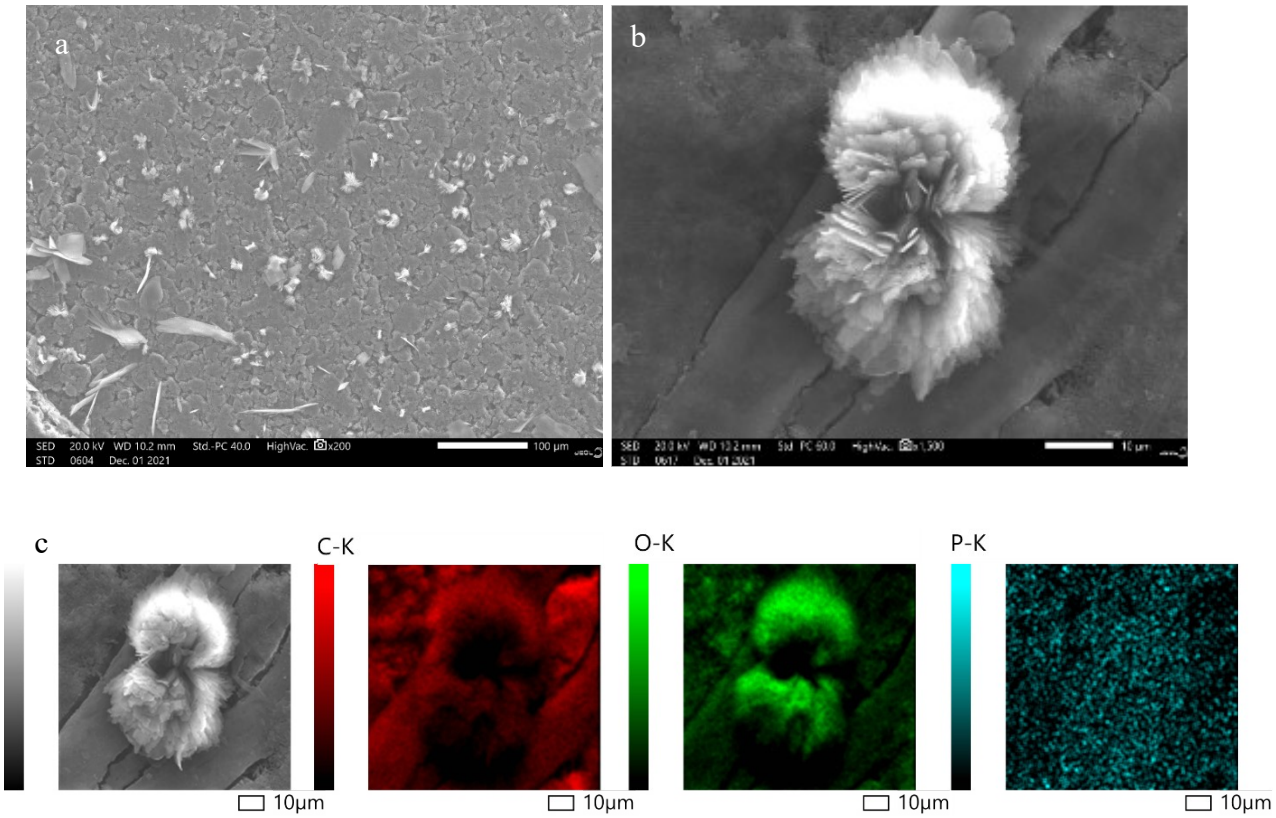

Figure S12. SEM image (a, and b) and EDS mapping (c) of the cycled electrode with M3 graphite. Before disassembly, all cells underwent rate tests lithiated to 90% SOC at 2C and were charged to 1.5 V.

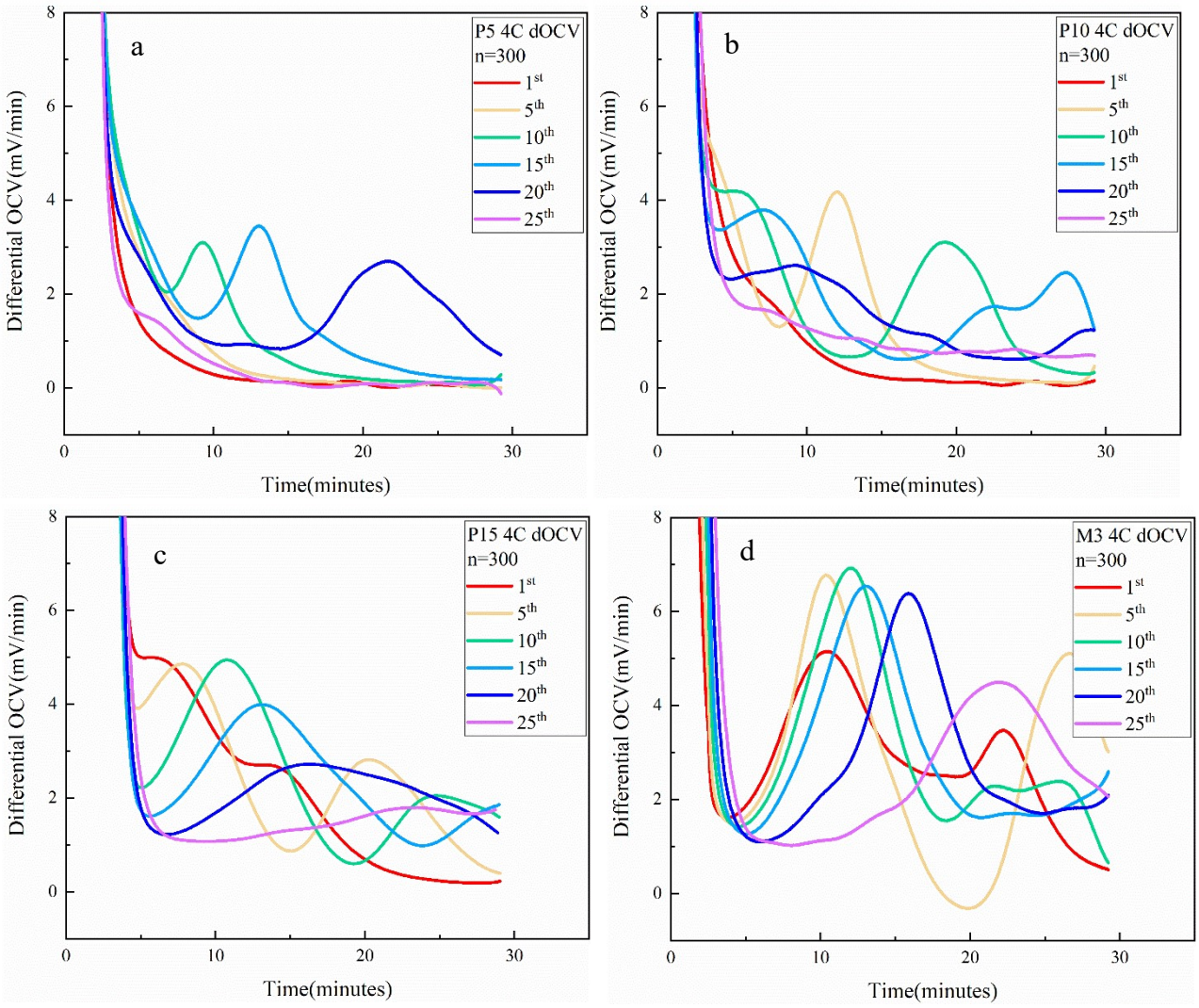

Figure S13. The differential OCV profiles of cells with P5 (a), P10 (b), P15 (c) and M3 (d) graphite anodes at various cycles. All cells were lithiated to 80% at 4C.

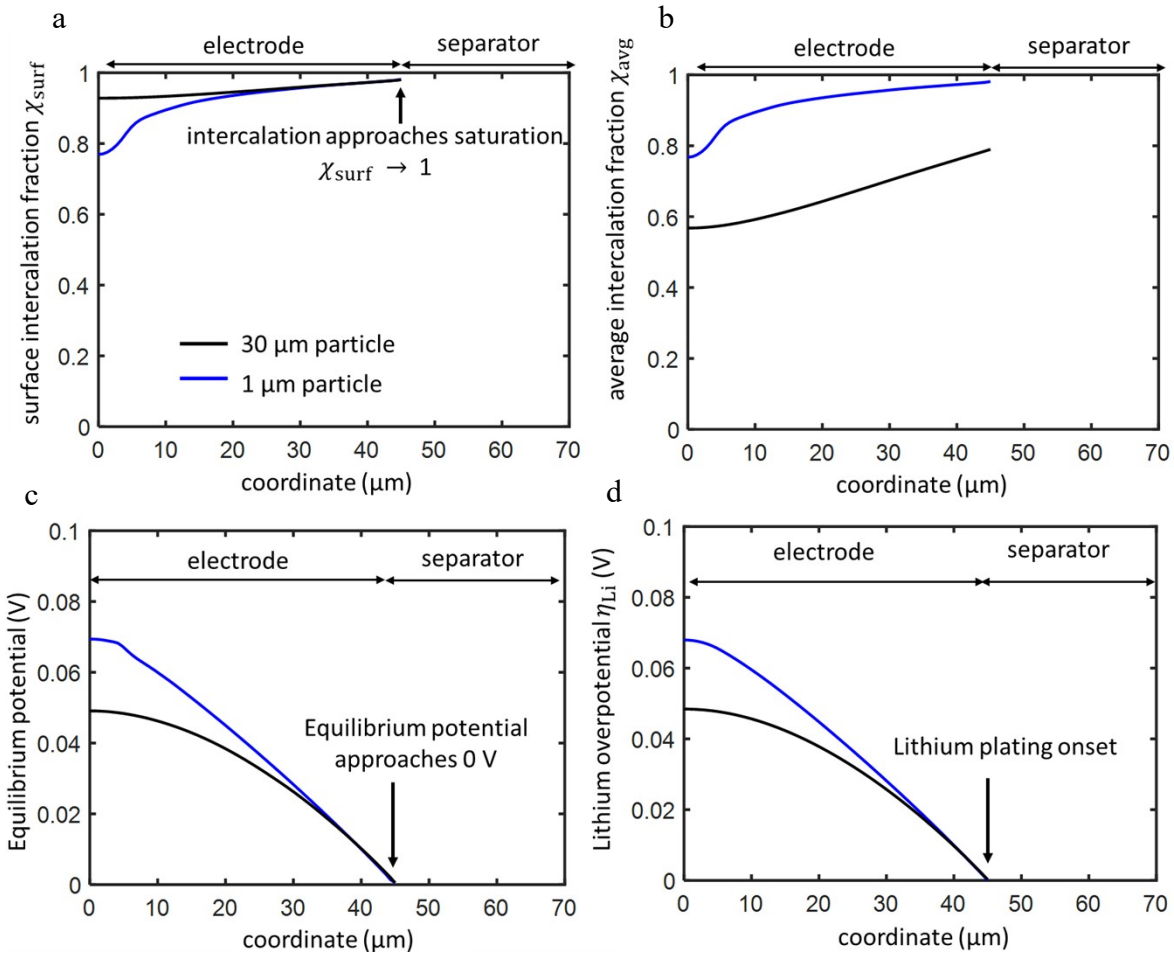

Figure S14. (a) Surface intercalation fraction, (b) average intercalation fraction, (c) equilibrium potential and (d) lithium overpotential as a function of coordinate for a 1 and 30 µm particle at plating onset for a 2C charge rate. Saturation of the particle surface (a) coincides with equilibrium potential approaching zero (c) and lithium overpotential approaching zero (d) at the electrode-separator interface.

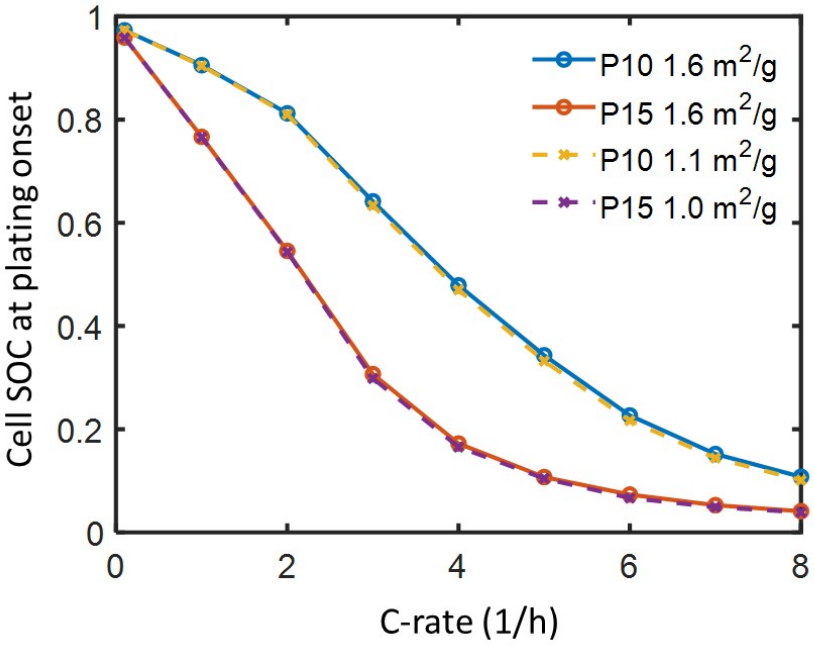

Figure S15: Cell state of charge at plating onset vs. C-rate for P10 and P15 graphite models with D90 particle size for various particle surface areas. The open circles correspond to the surface area of P5 (in m^2/g) whereas the crosses represent the surface area measured for the P10 and P15 materials. Changing surface area does not change onset of plating appreciably in these simulations. This comparison suggests that the particle size plays a larger role in plating onset than the particle surface area.

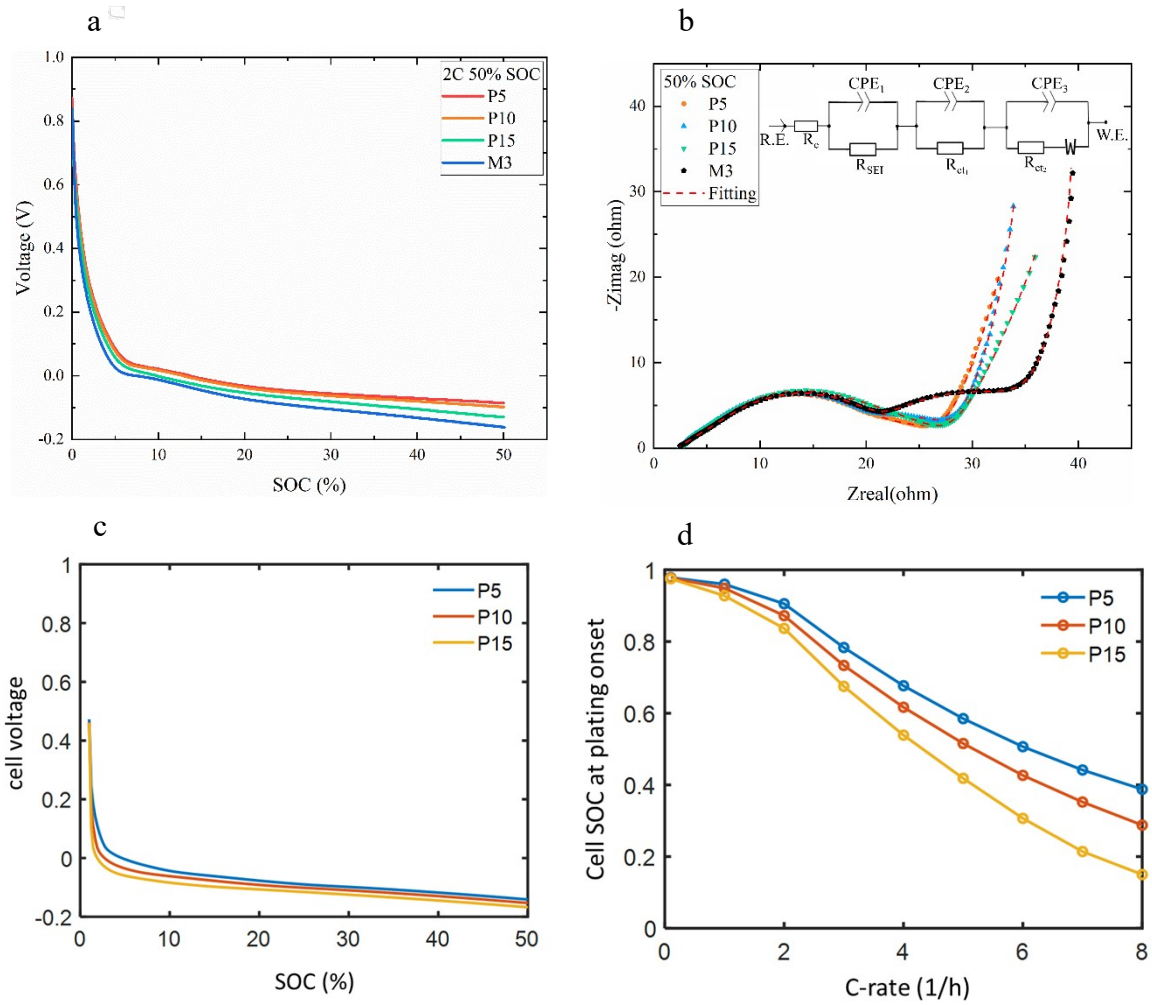

Figure S16. The experimental voltage profiles (a) of graphite electrodes with P5, P10, P15 and M3 lithiated to 50% SOC at 2C. The Nyquist plots (b) of graphite electrodes lithiated to 90% SOC and inset is the equivalent circuit used for data fitting. Theoretically predicted voltage curves (at 2C) (c) and capacities at plating threshold (d) as a function of C rate with various graphite electrodes for electrodes with 45 µm thickness and particle size corresponding to D90 of the particle distribution for P5, P10 and P15.

Table S1. Resistances and tortuosity of electrodes with various graphite

Graphite electrode	R_{total} (Ω)	$R_{contact}$ (Ω)	R_{ion} (Ω)	Tortuosity (τ)
P5	5.2	2.0	9.6	4.1
P10	5.8	2.0	11.4	5.0
P15	6.6	2.0	13.8	5.7
M3	9.0	2.0	21.0	8.6

* R_{total} and $R_{contact}$ were extracted from **Figure S7**;

** τ and R_{ion} were calculated from equations (1) and (2)

Table S2: Graphite anode parameters in numerical model.

Parameter	Symbol	Value
Porosity	ϵ_e	35%
Active solid fraction	$1 - \epsilon_e$	92%
Particle diameter	a_r	P5: 6.5 µm (D50) & 12.2 µm (D90) P10: 9.6 µm (D50) & 19.3 µm (D90) P15: 14.6 µm (D50)& 35.3 µm (D90) Mechanism study: 1 μm or 30 μm
Active specific surface area	a	P5: 3.52 × 10^6 1/m P10: 2.42 × 10^6 1/m P15 2.2 × 10^6 1/m Mechanism study: 3.52 × 10^6 1/m
Tortuosity	τ	5.5
Equilibrium potential (V)	E_{eq}	Fig. S12
Electrical conductivity	σ	100 S/m
Solid phase Li^+ diffusivity	D_s	1.45 × 10^{-13} m^2/s
Maximum concentration of Li in anode	c_s^{max}	29047
Initial intercalation fraction		0.01
Maximum intercalation fraction		1
Anodic exchange current density	i_0	$i_0 = Fkc^{0.5}\left(c_s^{max} - c_s\right)^{0.5} c_s^{0.5}$
Reaction rate constant	k	P5, P10, P15: 1 × 10^{-10} $\frac{m^{2.5}}{mol^{0.5}s}$ Mechanism study: 5 × 10^{-10} $\frac{m^{2.5}}{mol^{0.5}s}$
Anodic/Cathodic transfer coefficient	α_a/α_c	0.5

Table S3: Electrolyte parameters in numerical model.

Parameter	Symbol	Value
Initial salt concentration	c_o	1200 mol/m^3
Ionic conductivity	κ	See Figure S8
Li$^+$ diffusivity	D	
Effective ionic conductivity	κ_{eff}	$\kappa_{eff} = \kappa \times \frac{\epsilon_e}{\tau}$
Effective Li$^+$ diffusivity	D_{eff}	$D_{eff} = D \times \frac{\epsilon_e}{\tau}$
Activity coefficient	$\partial f_{\pm} / \partial \ln c$	See Figure S8
Transference number	t_+	See Figure S8

Table S4: Lithium metal electrode parameters in numerical model.

Parameter	Value
Exchange current density	8.5 A/m^2
Anodic transfer coefficient	0.5
Cathodic transfer coefficient	0.5
Equilibrium potential	0 V
Electrolyte reference concentration	1200 mol/m^3

Table S5. Summary of graphite information

Graphite	Particle size (D50, μm)	Particle size (D90, μm)	Specific surface area (m^2/g)
P5	6.5	12.2	1.6
P10	9.6	19.3	1.1
P15	14.6	35.3	1.0
M3	24.1	50.2	1.1

Table S6. Fitted values for the equivalent circuit elements by simulation of impedance spectra in **Figure S16b**

Graphite electrode	R_e (Ω)	R_{ct} (Ω)	R_{SEI} (Ω)
P5	2.4	20.2	2.9
P10	2.4	23.7	2.8
P15	2.3	24.4	2.7
M3	2.4	32.2	2.2